Surface Roughness Model and Process of Brazed Diamond Tool Milling and Grinding Sapphire Dome

FENG Wei[1*], *SUN Xiaokang*[1], *ZHANG Lingling*[2], *ZHU Nannan*[3]

1. School of Mechanical Engineering, Yancheng Institute of Technology, Yancheng 224001, P. R. China;
2. Qing Dao Haier Air Conditioner General Co., Ltd., Qingdao 266101, P. R. China;
3. Industrial Perception and Intelligent Equipment Engineering Research Center of Jiangsu Province, Nanjing University of Industry Technology, Nanjing 210023, P. R. China

(Received 24 March 2025; revised 16 June 2025; accepted 1 July 2025)

Abstract: Sapphire hemispherical domes are machined through milling and shaping using brazed diamond tools. A mathematical model describing roughness for this processing method is established, and the relationship between roughness and its influencing factors is analyzed. Experiments on the hemispherical dome shaping process are conducted to validate the model, analyzing the variation in roughness under different tool and workpiece rotational speeds. The results are consistent with the predictions of the established roughness model, suggesting that the model can be used to guide subsequent process experiments. Milling and shaping efficiency using brazed diamond tools typically can reach 14 g/min. The machined sapphire surfaces exhibit relatively few microcracks and minimal damage, with almost all exclusively visible grooves resulting from brittle fracture removal. The surface roughness after machining is below 2.5 μm. Milling sapphire domes with brazed diamond tools represents a novel shaping technique characterized by high efficiency and high quality.

Key words: diamond tools; sapphire dome; milling and grinding; roughness

CLC number: TG71; TG66 **Document code:** A **Article ID:** 1005-1120(2025)04-0554-11

0 Introduction

An external infrared fairing must be installed to protect the internal detection and optoelectronic systems of new missiles from damage. An infrared fairing, a key component of the missile weapon system[1], must possess excellent comprehensive properties in terms of optics, mechanics, physics, and chemistry[2-4]. Compared with other infrared optical materials, sapphire offers multiple advantages, including high hardness, superior mechanical strength, thermal shock resistance, and a low scattering coefficient[5-7], making it one of the most suitable materials for modern fairing applications. Furthermore, the gradual maturation of sapphire crystal growth technologies and the advancement of thermal imagers have rapidly expanded the application prospects of sapphire fairings[8-10]. Demand is increasing significantly, particularly for hemispherical fairings, which represent the most widely used configuration.

Sapphire infrared fairings are mostly formed using near-net-shape processing techniques, whereby 〈0001〉 crystal-oriented sapphire fairings are grown directly from the melt. Refs.[11-13] previously adopted methods such as non-capillary shaping (NCS), local dynamic shaping (LDS), and grown-from-an-element-of-shape (GES) strategies for developing sapphire infrared fairings. However, the direct growth of sapphire fairings faces certain limitations in terms of quality and thickness, and reports on alternative methods are rare. Domestically, Xu et al.[14-15] used external cylindrical grinding ma-

*Corresponding author, E-mail address: zhu5411492@163.com.

How to cite this article: FENG Wei, SUN Xiaokang, ZHANG Lingling, et al. Surface roughness model and process of brazed diamond tool milling and grinding sapphire dome[J]. Transactions of Nanjing University of Aeronautics and Astronautics, 2025,42(4):554-564.

http://dx.doi.org/10.16356/j.1005-1120.2025.04.010

chines in combination with precision grinding moulds to assist in the machining of sapphire fairings, obtaining fairings with good surface quality. Wang[16] performed conformal fairing grinding of sapphire on an ultra-precision machine tool. Both the inner and outer surfaces were ground with a spherical grinding wheel. The wheel underwent online dressing and measurement during the process, with the real-time wheel radius compensated into the machine tool trajectory. Pan[17] summarised the processing methods and quality control techniques for sapphire infrared fairings based on experimental studies involving the speed and pressure of fine grinding and polishing machines, materials of the fine grinding mould layers, polishing films, polishing agents, as well as jigs and fixtures. However, all these methods face challenges in achieving both high efficiency and high quality simultaneously. Currently, the more efficient method for shaping sapphire is the so-called "fishing ball" method, which uses milling cutters for cutting and shaping. In this paper, an innovative approach is explored based on the "scooping-ball" process. Specifically, brazed diamond tools are employed for milling and shaping sapphire crystal rods[18]. A model of the surface roughness of workpieces formed through this processing method is established, and the fundamental rules of milling and shaping are derived, aiming to obtain high-quality fairings. This approach provides a foundation for subsequent grinding and polishing processes and offers reference data for setting process parameters in the shaping of other optical domes.

1 Machining Principle and Roughness Model

1.1 Machining principle

The workpiece blank is a directly grown single-crystal sapphire crystal rod, which is formed into a hemispherical shape. Due to the material's inherent properties, the form of the tool adopt a hemispherical bowl-shaped tool base. The base dimensions are shown in Fig.1. Diamond particles are brazed onto the upper end of the base, more than 6 mm above, for shaping processing. Fig.2 shows a photo of the brazed diamond tool. The vacuum brazing process is used, with temperature rise controlled at 8 ℃ per minute, reaching a maximum temperature of 1 000 ℃. The braze material is a Ni-Cr based alloy, and the diamond particle size ranges from 30 mesh to 50 mesh. The workpiece forming principle diagram uses a blank with a diameter of 50.6 mm and a length of 100 mm. The tool and workpiece rotate around their own axes, and the tool moves along the trajectories indicated by the dashed lines 1 and 2 in the Fig.1. The processed sapphire dome has a thickness of 5 mm, an inner diameter of 42 mm and an outer diameter of 52 mm. To process hemispherical domes of other sizes, only the corresponding size of the tool needs to be replaced.

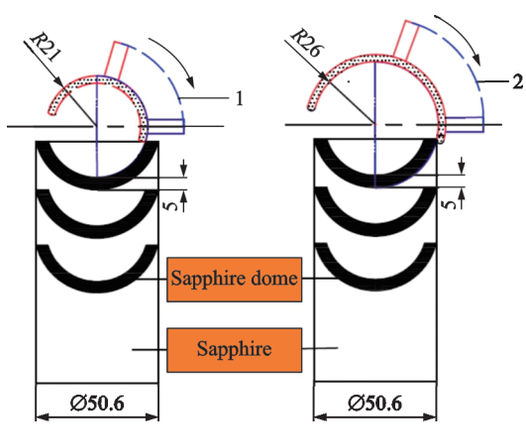

Fig.1 Machining schematic diagram

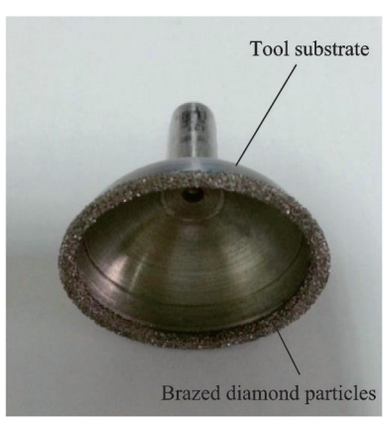

Fig.2 Milling and grinding tool photo

1.2 Roughness model

The size of the surface roughness formed on the workpiece after processing is related to the

shape of the material removal corresponding to the processing method. Since the spherical dome forming tool head mentioned above adopts a single-layer brazed diamond tool, the shape of the abrasive grain is preliminarily simplified and assumed to be an octahedron, i.e. the shape of the exposed part participating in the processing is a square pyramid.

Based on the motion form of the spherical cap forming process, to facilitate more intuitive analysis and calculation, the geometric diagram of the abrasive particle cutting-in is magnified several times in a small area, resulting in the geometric model of abrasive particle cutting-in and material removal in spherical dome forming process as shown in Fig.3. The black shaded area in the figure represents the sapphire workpiece material remaining between two abrasive particles after a single spherical dome forming process under ideal conditions. This is mainly due to the existence between the abrasive particles during the brazing process and is related to the shape of the abrasive particles.

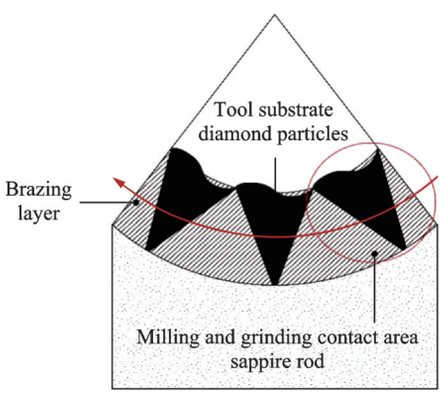

Fig.3 Geometric model of material removal for dome milling and grinding

To analyze the surface roughness of the workpiece, the following assumptions are made:

(1) The abrasive particles are evenly distributed on the surface of the ball cover forming tool, with the same protruding height.

(2) The tool has no wear on single cuts, and the impact on processing equipment can be disregarded.

(3) The removal of scratches is produced without overlap.

According to the research of relevant scholars on roughness, it is found that for this type of diamond abrasive grains in the actual processing, it is simpler to further assume the shape and size as spherical equivalent particle size, which is also closer to the actual situation[19-20]. Therefore, in this study, when discussing roughness, the diameter of the circle circumscribed around the above-mentioned octahedral diamond abrasive grains is further defined as the equivalent particle size D'[21]. If the edge length of the octahedral abrasive grain is a, the relationship with the equivalent particle size is

$$a=\frac{\sqrt{\pi}}{2}D' \tag{1}$$

Assuming that a single abrasive grain is subjected to a force of F_p, the depth h pressed into the sapphire surface can be calculated as

$$h=\left[\frac{9\pi^2F_p^2(k'+k'')}{16rR}\right]^{\frac{1}{3}} \tag{2}$$

where $k'=\frac{1-\mu_1^2}{\pi B_1}$, $k''=\frac{1-\mu_2^2}{\pi B_2}$, r is the equivalent radius of the abrasive grain, and R the equivalent radius of the bowl shaped tool. Due to the fact that the former is much smaller than the latter (the diameter size of bowl shaped tools is generally between 40 mm and 80 mm), the above equation can be simplified as

$$h=\left[\frac{9\pi^2F_p^2(k'+k'')}{16r}\right]^{\frac{1}{3}} \tag{3}$$

Then $\frac{h}{r}=\left[\frac{9\pi^2F_p^2(k'+k'')}{16r^4}\right]^{\frac{1}{3}}$.

According to Eq.(1), we have

$$r=\frac{a}{\sqrt{\pi}} \tag{4}$$

$$\frac{h}{r}=\left[\frac{9\pi^2F_p^2(k'+k'')}{16a^4}\right]^{\frac{1}{3}} \tag{5}$$

In a small-scale range, a curved surface can be approximated as a plane. As shown in Fig.4, it is the geometric model of the roughness of the spherical dome forming. The x-x line represents the profile centerline of the spherical dome forming surface. Before calculating the roughness Ra, it is necessary to first determine the value of y.

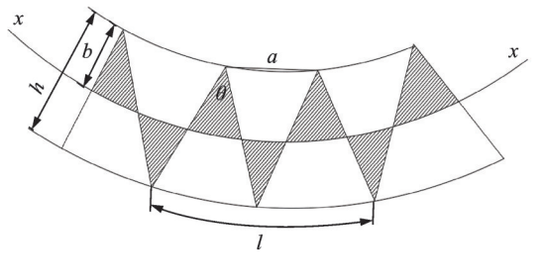

Fig.4 Schematic diagram of the average deviation of the milling and grinding section profile of the dome

According to geometric calculations, we have

$$l=2\sqrt{\frac{2ah}{\sqrt{\pi}}-h^2} \tag{6}$$

$$A_{\mathrm{T}}=y^2\cot\frac{180-\theta}{2} \tag{7}$$

$$A_{\mathrm{B}}=\frac{1}{2}hl-\frac{y}{2}\left(2l-2y\cot\frac{180-\theta}{2}\right) \tag{8}$$

where A_{T} and A_{B} are the areas of the shaded areas on the x-x center line and below the two triangles in Fig.4, respectively. Since x-x is the contour centerline, y can be calculated as

$$y=\frac{1}{2}h \tag{9}$$

According to the definition of Ra, it can be inferred that

$$Ra=\frac{\sqrt{3}}{2}\left[\frac{9\pi^2F_{\mathrm{p}}^2(k'+k'')}{16r}\right]^{\frac{1}{3}} \tag{10}$$

For the formation of ball covers, in a single machining process (without changing the machining process parameters), the pressure p used by the entire tool along the feed direction is constant, and the force on a single abrasive particle is related to the average number of abrasive particles in contact per unit area. Given a coefficient of m, then

$$F_{\mathrm{p}}=m'\frac{p}{v_{\mathrm{d}}v_{\mathrm{s}}12.5\dfrac{\pi R\varphi}{180}}=m\frac{p}{v_{\mathrm{s}}v_{\mathrm{d}}\varphi} \tag{11}$$

where v_{s} is the rotational speed of the sapphire rod; v_{d} the rotational speed of diamond brazed tools; φ the entrance angle; and m' a coefficient related to the structure, namely $m=\dfrac{m'}{12.5\dfrac{\pi R}{180}}=14.4\dfrac{m'}{\pi R}$.

The roughness model of the ball cover forming process obtained by substituting Eq.(11) into Eq.(10) is

$$Ra=\frac{\sqrt{3}}{2}\left[\frac{9\pi^2m^2p^2(k'+k'')^2}{16rv_{\mathrm{s}}v_{\mathrm{d}}\varphi^2}\right]^{\frac{1}{3}} \tag{12}$$

It can be seen that the surface roughness of sapphire after milling and grinding is related to the force on a single abrasive particle, the equivalent radius of the abrasive particle, the rotational speed of the tool, and the rotational speed of the workpiece. To quantify the relationship between the roughness value and each parameter and establish the intersection domain with the cutting force model, a single parameter group is pre-tested and substituted to obtain an approximate value. The expected work to be achieved is the surface roughness value of the workpiece $Ra\leqslant 5$ μm, thus $v_{\mathrm{s}}v_{\mathrm{d}}\geqslant 57\,500$. To ensure the quality of the workpiece surface after milling and grinding, when conducting process experiments, the parameter selection range should be the intersection of the values that are both optimal for force and roughness conditions, that is

$$\{F_{\mathrm{p}}v_{\mathrm{s}}/v_{\mathrm{d}}<1\,260\}\cap\{v_{\mathrm{s}}v_{\mathrm{d}}\geqslant 57\,500\} \tag{13}$$

In conclusion, due to the high cost of sapphire crystal rods, in order to maximize the yield of spherical domes, the selection of process parameters in the subsequent process experiments will be within the intersection range as shown in Eq.(13). This is to avoid the waste and damage of raw materials caused by unreasonable parameter settings.

2 Experiment

The experimental equipment and clamping system are the self-made sapphire hemispherical dome processing equipment made by the research group. The inner side, outer side and end of the hemispherical dome forming tool's cutting head are respectively brazed with a layer of 40-mesh diamond particles at high temperature. The inner diameter of the tool body is 52 mm and the outer diameter is 60 mm. During the processing, the coolant flows through the rotating processing area under the action of centrifugal force, with a flow rate of 100 ml/min. The coolant is a 3% ethylene glycol water solution.

The workpiece to be processed is a single crystal sapphire rod with a diameter of 2″ and a length of

100 mm. The sapphire rod is clamped in a three-jaw chuck and rotated by the motor spindle. During the processing, the tool rotates around the axis of the tool holder and swings around the center of the large pulley driven by the transmission block. The surface roughness of the processed surface is measured by a TR220 portable roughness meter from Mahr. The roughness measurement length is 0.25 mm. The measurement result is the average value of the roughness of 20 points on the processed surface. The three-dimensional topography of the workpiece surface after processing is tested by a Keyence optical microscope system. The morphology of the sapphire surface, tool and chips after processing is observed by a scanning electron microscope (SEM). The specific process parameters of the equipment operation are shown in Table 1. The experimental equipment is shown in Fig.5.

Table 1 Process parameters for dome forming experiment

Parameter	Workpiece rotation speed/ ($r \cdot min^{-1}$)	Tool speed/ ($r \cdot min^{-1}$)
1	600	180
		230
		270
		300
2	225	270
	375	
	525	
	675	

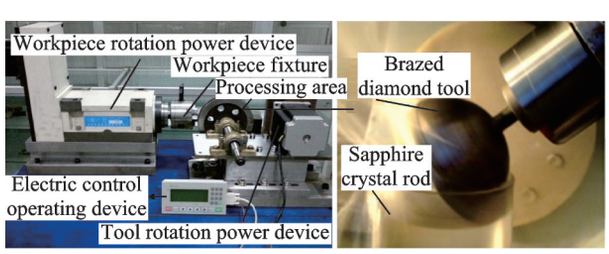

Fig.5 Photo of experimental equipment

3 Results and Discussion

3.1 Relationship between surface roughness and process parameters

The surface roughness of the machined sapphire is measured using a portable roughness tester. For each set of process parameters, 20 measurement points are selected, with the measurement direction at each point kept perpendicular to the machined surface of the workpiece. For each process condition, the roughness value is assumed as the average of six measurements. Fig.6 plots the variation curves of the surface roughness of sapphire after machining under different process conditions. As shown in Fig.6(a), the workpiece rotational speed is maintained at a constant of 600 r/min, while the tool rotational speeds are 180, 230, 270, and 300 r/min. The surface roughnesses of the machined sapphire hemisphere decrease with the increase in the rotational speed of the bowl-shaped tool, mainly because as the tool rotational speed increases, the distance between the milling trajectories generated by the brazed diamond grits at the tool tip on the workpiece surface decreases, leading to a higher trajectory density. Consequently, the surface roughness of the machined sapphire is reduced.

As shown in Fig.6(b), the tool rotational speed is maintained at a constant of 270 r/min,

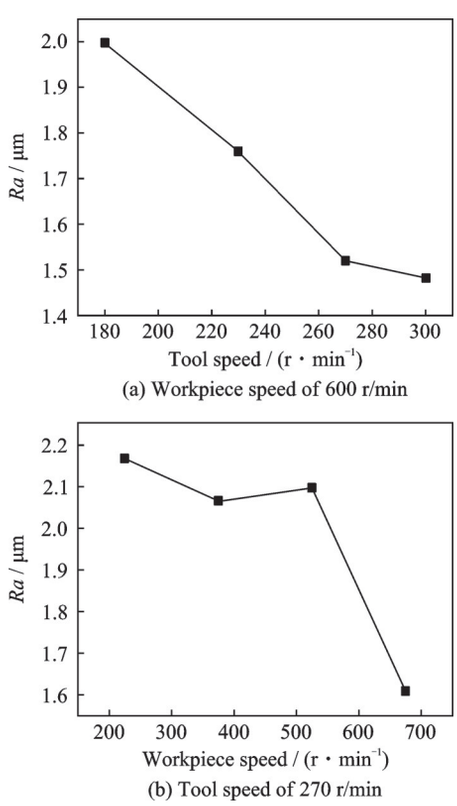

Fig.6 Surface roughness variation curves

while the workpiece rotational speeds are 225, 375, 525, and 675 r/min. The surface roughnesses of the machined sapphire hemisphere decrease with increasing workpiece rotational speed. Thus, in the milling and shaping of sapphire hemispherical domes, both the rotational speed of the bowl-shaped tool and the rotational speed of the sapphire crystal rod significantly influence the surface roughness of the machined sapphire hemisphere. Under the preset process parameters, the average surface roughness of the machined sapphire hemisphere is approximately 1.7 μm.

Therefore, for milling and shaping sapphire hemispherical domes using brazed diamond tools, the surface roughness of the machined workpiece is dependent on both the tool and workpiece rotational speeds. An increase in the rotational speed of the brazed diamond tool leads to a decrease in roughness; likewise, an increase in the rotational speed of the sapphire crystal rod also results in reduced roughness. Compared with Eq.(12) of the roughness model established in the previous section, when the workpiece rotational speed is held constant and the tool rotational speed is increased, the roughness decreases; when the tool rotational speed is held constant and the workpiece rotational speed is increased, the roughness also decreases, consistent with the predictions of the proposed model.

3.2 Analysis of processing efficiency

In conventional cylindrical grinding, the machined object is always cylindrical. Therefore, calculating the removal rate is relatively simple, dependent only on the external cylindrical diameter of the workpiece, the workpiece rotational speed, grinding depth, and feed rate. However, for milling and shaping sapphire hemispherical domes using the new equipment, the arc length of the cutting edge of the brazed diamond tool in contact with the workpiece constantly changes during the process due to the particular characteristics of the tool motion, tool type, and workpiece shape. Moreover, when the first dome is formed on an unprocessed sapphire crystal rod, the final removed portion is a spherical cap corresponding to the inner diameter of the tool. Thus, the traditional concept of removal rate does not apply to this processing method. The milling and shaping efficiency of dome machining, denoted as M_L, is defined as the mass removed per unit time.

$$M_L = M_Q / t \tag{14}$$

where M_Q represents the removed mass and t the time taken for the removal. Due to the difference in the shape and mass of the material removed when milling and grinding the first spherical dome compared with the second, third, and subsequent ones on a single crystal rod. The removed mass M_Q specifically refers to the loss of workpiece material caused by the direct contact of the tool's cutting edge.

Fig.7 presents the variation in machining efficiency during the milling and grinding of sapphire hemispherical domes. The workpiece rotational speed is fixed at 600 r/min, while the tool rotational speeds are 180, 230, 270, and 300 r/min. The machining efficiency increases with increasing tool speed (Fig.7(a)) because, under a constant workpiece speed, the number of times the tool contacted and milled/ground the workpiece per unit time increases. Accordingly, the material removal rate also increased[22]. When the tool rotational speed is fixed at 270 r/min, and the workpiece rotational speeds are 225, 375, 525, and 675 r/min, the milling and shaping efficiencies also increase with increasing workpiece speed, as shown in Fig.7(b), mainly because when the workpiece rotational speed increases, the relative velocity between the spherical surface material and the tool also increases, lengthening the cutting path per tool engagement. Under the same feed conditions, the area of material involved in cutting per unit time increases, thereby enhancing the material removal rate. Overall, the milling and shaping efficiencies using brazed diamond tools generally exceed 14 g/min. Considering the sapphire crystal rods used in the experiments as examples, with a diameter of 50.8 mm and a length of 100 mm, the time required to shape the first spherical surface is approximately 90 min, and the time to

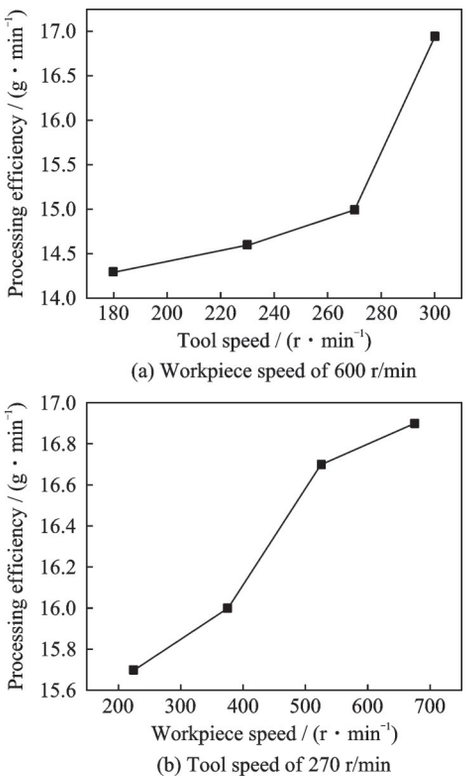

Fig.7 Efficiency variation curves of milling and grinding processing

machine the first complete hemispherical dome is approximately 120 min. The average time required for machining subsequent domes is approximately 40 min. The machined surface achieves a roughness *Ra* of less than 2.5 μm. Currently, processing methods capable of achieving such dome quality include direct growth techniques such as NCS, which typically require several days to grow a single dome and demand a high level of technical expertise, as previously discussed. Therefore, this study takes sapphire as the raw material, and uses brazing diamond tools to mill-grind the sapphire dome, which is an efficient processing.

3.3 Surface analysis of sapphire after milling and grinding

As shown in Fig.8(a), a SEM image, magnified 100 times, displays the surface of a sapphire workpiece milled using brazed diamond tools under process parameters of a workpiece rotational speed of 675 r/min and a tool rotational speed of 275 r/min. The surface exhibits uneven patterns caused by friction and extrusion from the brazed diamond grits, inducing compressive and shear stresses that leave scratch marks in the form of grooves on the workpiece surface. Further magnification of the machined sapphire surface to 500 times, as shown in Fig.8(b), reveals relatively few microcracks and damage. The visible surface features are almost exclusively grooves formed by brittle material removal, attributed to the use of bowl-shaped tools with diamond grits brazed at high temperatures, which enhances grit retention. Consequently, grit detachment is rare, and the diamond grits maintain an excellent cutting performance throughout the process. The machining operation remains stable, significantly reducing surface quality degradation typically caused by grit dislodgement or excessive friction from redundant grits. Furthermore, the orderly arrangement of diamond micro-edges increases both heat dissipation capacity and chip accommodation space, which further improves the surface quality. Thus, workpieces with a certain level of surface quality are obtained. Fig.9 presents a three-dimensional morphology image of a sapphire surface after milling with a brazed diamond tool. Subsequent grinding and polishing processes are necessary to achieve even better surface quality.

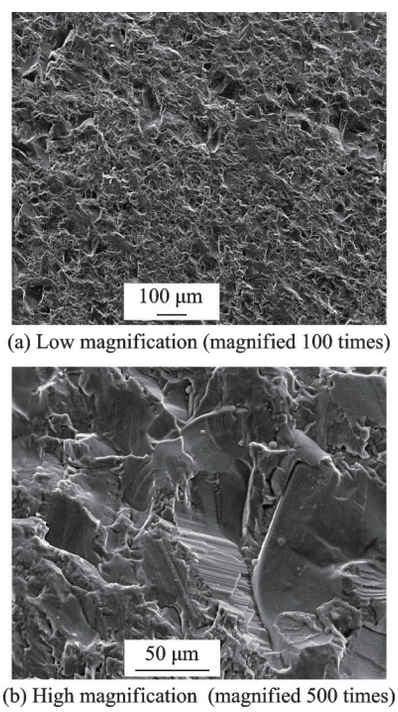

Fig.8 SEM images of sapphire surface after milling and grinding

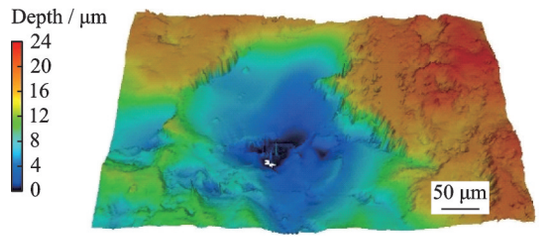

Fig.9 Three-dimensional morphology of sapphire surface after milling and grinding

As shown in Fig.10, a morphology image of the sapphire surface after machining is captured using a hand-held microscope at 200 magnification after the machined workpiece has undergone ultrasonic cleaning in alcohol for 6 h. Despite the cleaning, a large amount of milling and grinding swarf remains within the groove-like trajectories on the machined surface. The milling and grinding swarf generated during the process is small in volume and tends to fall into the voids formed during machining. As its composition is the same as the base material, the swarf adheres strongly, making it difficult to remove.

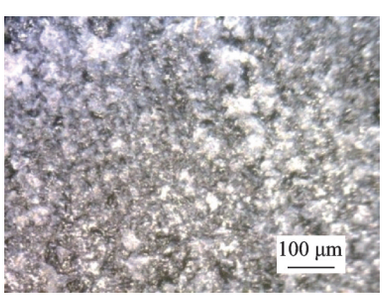

Fig.10 Microscopic image of processed sapphire

The collected milling and grinding swarf is analysed by energy-dispersive X-ray spectroscopy (EDS), with the elemental composition shown in Fig.11. The main elements are aluminium (66.58%) and oxygen (26.87%), which correspond to the sapphire material itself. In addition, small amounts of chromium, iron, and nickel are detected, attributed to the binder components of the brazed diamond grits in the tool. After a period of milling and shaping, the cutting forces cause tool wear. During this interaction, small amounts of binder and even grits may detach and mix with the removed material.

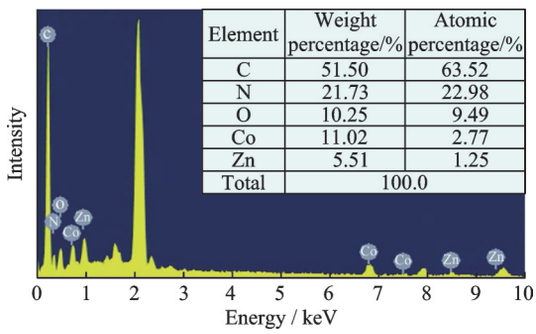

Element	Weight percentage/%	Atomic percentage/%
C	51.50	63.52
N	21.73	22.98
O	10.25	9.49
Co	11.02	2.77
Zn	5.51	1.25
Total	100.0	

Fig.11 EDS image of milling

Fig.12 presents SEM images of the swarf morphology. In Fig.12(a), magnified 500 times, the milling and grinding swarf appears as fragmented chips, and the undispersed chip agglomerates are relatively small in size. At a magnification of 800 times (Fig.12(b)), in addition to fragmented chips, a ribbon-like morphology is also observed at the microscale, suggesting that when milling single-crystal sapphire (a brittle and hard material) with a brazed diamond bowl-shaped tool, continuous plastic chips may also be produced in addition to brittle fracture particles. Combined with the surface roughness measurements discussed above, higher tool rotational speeds lead to lower surface roughness values on the sapphire hemisphere, indicating that the

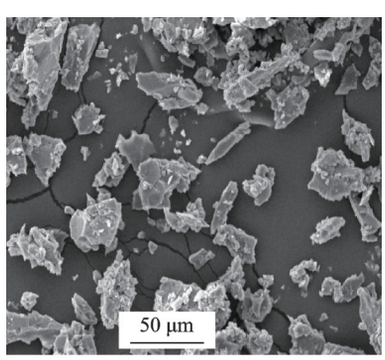

(a) Magnification of 500 times

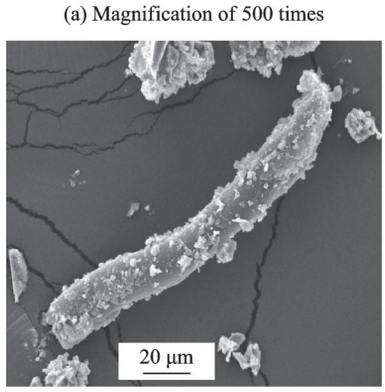

(b) Magnification of 800 times

Fig.12 SEM images of sapphire removal material

increase in machining speed may result in a change in the chip formation mechanism. In summary, using brazed diamond bowl-shaped tools can typically achieve a milling and shaping efficiency exceeding 14 g/min. The processing time for a single sapphire dome is significantly shorter than traditional dome growth methods. Moreover, due to the controllable grit size of brazed diamond particles, a brittle-to-ductile transition may occur during machining. The machined surface roughness Ra can be reduced to below 2.5 μm. Therefore, using brazed diamond tools for milling and shaping sapphire domes represents an ideal hemispherical dome-shaping process. The resulting surface quality of the workpiece is high, reducing the difficulty of subsequent grinding and polishing, thereby improving the overall processing efficiency.

4 Conclusions

(1) A roughness model for the milling and grinding forming of sapphire hemispherical domes with brazed diamond tools is established. The roughness is related to the force on a single abrasive grain, the equivalent radius of the abrasive grain, the rotational speed of the tool, and the rotational speed of the workpiece.

(2) The results of hemispherical dome-shaping experiments show that increasing the rotational speed of the brazed diamond tool leads to a decrease in surface roughness. Similarly, increasing the rotational speed of the sapphire crystal rod also reduces surface roughness. A comparison with the established roughness model confirms that with constant workpiece rotational speed, an increase in tool speed reduces surface roughness. Likewise, with constant tool speed, increasing the workpiece rotational speed also reduces surface roughness. These experimental results are consistent with model predictions, which can help guide the selection of process parameters in future experiments.

(3) The processing efficiency increases with the rise of tool speed and workpiece speed. The milling and grinding forming efficiency using brazed diamond tools can generally reach over 14 g/min. Therefore, using brazed diamond tools for milling and grinding sapphire hemispherical domes is an efficient forming processing method.

(4) The machined sapphire surfaces have relatively few microcracks and damage. Visible features predominantly consists of grooves formed by brittle fracture removal. A considerable amount of milling swarf remains in the groove-like tracks on the machined surface. The main elemental components are aluminum, oxygen, and trace amounts of iron, chromium, and nickel. The milling and grinding swarf exhibits a chip-like morphology, with a microstructure resembling ribbon-shaped chips. Milling single-crystal sapphire (a brittle and hard material) using brazed diamond bowl-shaped tools may generate continuous plastic milling chips in addition to brittle fracture particles. The surface roughness Ra after machining is below 2.5 μm.

References

[1] GAO Y X, WANG Y Y, LIU S Y, et al. Preparation of paraffin wax-modified floating aluminum powder and composite coating with infrared stealth and wave-transparent function[J]. Materials Science and Engineering: B, 2023, 295: 116611.

[2] LI Fuwei, ZHAO Hongxia, PAN Guoqing, et al. Research on the characteristics of high strength nano infrared ceramic fairings for medium wave infrared missiles[J]. Acta Optica Sinica, 2021, 41(3): 1-6. (in Chinese)

[3] PANG Chuanbo, XIANG Yuwei, MA Xingpu, et al. Research on the aerodynamic characteristics of hypersonic missile inlet fairing separation[J]. Journal of Missile and Guidance, 2020, 40(3): 123-134. (in Chinese)

[4] KWON S B, NAGARAJ A, XI D L, et al. Studying crack generation mechanism in single-crystal sapphire during ultra-precision machining by MD simulation-based slip/fracture activation model[J]. International Journal of Precision Engineering and Manufacturing, 2023, 24(5): 715-727.

[5] LI S P, FU J N, HE Z B, et al. Nanomaterials and equipment for chemical-mechanical polishing of single-crystal sapphire wafers[J]. Coatings, 2023, 13(12): 2081.

[6] LI Z C, PEI Z J, FUNKENBUSCH P D. Machining processes for sapphire wafers: A literature review[J]. Proceedings of the Institution of Mechanical Engi-

neers, Part B: Journal of Engineering Manufacture, 2011, 225(7): 975-989.

[7] WANG Zhangkui, HUANG Shangci, LIU Kuncheng, et al. Lapping of sapphire using developed clusters of diamond and ceria chemically active abrasives[J]. Materials Today Communications, 2024, 39: 109386. (in Chinese)

[8] DONGHAI W, LI D Z, XU J. An important breakthrough in the technology of sapphire plate with large size grown by the edge-defined film-fed growth method[J]. Journal of Inorganic Materials, 2023, 38(3): 363-364.

[9] VOROB'EV A, KALAEV V, MAZAEV K. Chemical model of sapphire crystal growth by Ky technique[J]. Journal of Crystal Growth, 2023, 612: 127196.

[10] BAKHOLDIN S I, KRYMOV V M, NOSOV Y G. Calculation of residual stresses in shaped sapphire single crystals from conoscopic measurement data[J]. Technical Physics, 2021, 66(4): 535-542.

[11] HARRIS D C. A peek into the history of sapphire crystal growth[C]//Proceedings of Window and Dome Technologies Ⅷ. Orlando, FL: SPIE, 2003.

[12] HOROWITZ A, BIDERMAN S, EINAV Y, et al. Improved control of sapphire crystal growth[J]. Journal of Crystal Growth, 1996, 167(1/2): 183-189.

[13] ANTONOV P I, KURLOV V N. A review of developments in shaped crystal growth of sapphire by the Stepanov and related techniques[J]. Progress in Crystal Growth and Characterization of Materials, 2002, 44(2): 63-122.

[14] XU Yan, LI Caishuang, SUN Qiang. Research on manufacturing technology of hemispherical sapphire fairing[J]. Optical technology, 2006, 32(4): 636-638. (in Chinese)

[15] LIANG Chao. Optimization and experimental study on processing technology of large-size sapphire fairing[D]. Harbin: Harbin University of Science and Technology, 2013. (in Chinese)

[16] WANG Jinhu. Research of key technology on precision grinding of deep conformal sapphire dome[D]. Harbin: Harbin Institute of Technology, 2018. (in Chinese)

[17] PAN Guoqing. Development and performance testing of large diameter sapphire half spherical infrared fairings[C]//Proceedings of 2006 Academic Conference of the Chinese Optical Society. Guangzhou, China: Chinese Optical Society, 2006: 412-413. (in Chinese)

[18] LOCHER J W, BATES H E, JONES C D, et al. Producing large EFG sapphire sheet for VIS-IR (500—5 000 nm) window applications[C]//Proceedings of Window and Dome Technologies and Materials Ⅸ. Orlando, Florida, USA: SPIE, 2005.

[19] LAL G K, SHAW M C. Wear of single abrasive grain in fine grinding[C]//Proceedings of the International Grinding Conference. Pittsburgh, USA: Carnegie Press, 1972.

[20] ZHANG Lu, LI Weilong, WANG Yuzhuo, et al. Effect of broaching machining parameters on low cycle fatigue life of Ni-based powder metallurgy superalloy at 650 ℃[J]. Transactions of Nanjing University of Aeronautics and Astronautics, 2023, 40(5): 511-521.

[21] CHEN Changzheng, WU Huanjie, LI Ying, et al. Finite element simulation and analysis of single particle diamond grinding SiC ceramics[J]. Journal of Shenyang University of Technology, 2022, 44(2): 180-184. (in Chinese)

[22] LIU Mingmiao. Mechanical engineering design, preparation, and experimental study of brazed diamond tools for efficient drilling of hard and brittle ceramics[D]. Yangzhou: Yangzhou University, 2024. (in Chinese)

Acknowledgements This work was supported by the National Natural Science Foundation of China (No.51675457) and the Jiangsu Key Laboratory of Precision and Micro-manufacturing Technology.

Author

The first/corresponding author Dr. **FENG Wei** received the Ph.D. degree in mechanical manufacturing from Nanjing University of Aeronautics and Astronautics, Nanjing, China, in 2017. From 2017 to present, she has been with School of Mechanical Engineering, Yancheng Institute of Technology, Yancheng, China. Her research focuses on precision machining and ultra-precision machining.

Author contributions Dr. **FENG Wei** designed the study, complied the models, conducted the analysis, interpreted the results and wrote the manuscript. Mr. **SUN Xiaokang** contributed to data collection. Ms. **ZHANG Lingling** contributed to materials preparation. Prof. **ZHU Nannan** contributed to the background of the study. All authors commented on the manuscript draft and approved the submission.

Competing interests The authors declare no competing interests.

(Production Editor: XU Chengting)

钎焊金刚石工具铣磨加工蓝宝石球罩表面粗糙度模型及工艺

冯 伟[1]，孙孝康[1]，张玲玲[2]，朱楠楠[3]

（1.盐城工学院机械工程学院，盐城 224001，中国；2.青岛海尔空调器有限公司，青岛 266101，中国；
3.南京工业职业技术大学江苏省工业感知与智能装备工程研究中心，南京 210023，中国）

摘要：采用钎焊金刚石工具铣磨成形加工蓝宝石半球罩。建立了该工艺方法的粗糙度数学模型，分析了粗糙度值与其影响因素间的关系。为验证模型进行了半球罩成型工艺实验，分析不同工具转速及工件转速下粗糙度的变化，与所建立的粗糙度模型相吻合，模型可用于指导后期相关工艺实验。利用钎焊金刚石工具进行铣磨成形效率一般可达到 14 g/min，铣磨成形后的蓝宝石表面加工后表面的微观裂纹和损伤较少，几乎只可见材料脆性去除的沟痕。加工后的表面粗糙度达到 2.5 μm 以下。采用钎焊金刚石工具铣磨蓝宝石球罩是一种高效、高质量新型成形加工方式。

关键词：金刚石工具；蓝宝石球罩；铣磨；粗糙度